

Radiative Meson Decays in a Quark-Oscillator Model*

Steven B. Berger and Bernard T. Feld

Laboratory for Nuclear Science and Department of Physics, Massachusetts Institute of Technology, Cambridge, Massachusetts 02139

(Received 2 July 1973)

One- and two-photon decays of meson resonances are calculated in a quark-oscillator model using a nonrelativistic interaction Hamiltonian and vector dominance. Harmonic-oscillator wave functions are assumed for $l = 0$ and $l = 1$ resonances (e.g., π , ρ and A_2 , f , respectively). The calculations in general are sensitive to the value of the well-width parameter α^2 . Good agreement with experiment is obtained for decays of low-lying states (such as π^0 and η) and for the decay $A_2^+ \rightarrow \pi^+ + \gamma$ [Γ (predicted) = 0.4–0.6 MeV]. The calculated width for the decay $f(1260) \rightarrow \gamma\gamma$ is less than that predicted by Kunzst *et al.*, on the basis of a phenomenological Lagrangian by a factor of 3 or more.

Quark models have successfully been applied to obtain a basis for understanding the electromagnetic properties of baryonic and mesonic states.¹ The simplest of these models assumes that hadrons are made up of structureless "quarks" of three types: \mathcal{P} , \mathcal{N} , and λ with the quantum numbers given in Table I. (In Table I, B = baryon number, I = isospin, Y = hypercharge, S = strangeness, e_q = quark electric charge.)

For mesons, the work of Van Royen and Weisskopf² provides a basis for understanding electromagnetic properties and decays of mesonic states on the basis of the process illustrated in Fig. 1 for the transition $a \rightarrow b + \gamma$.

For the case in which a (b) is a vector meson (quark-antiquark pair in the 3S_1 state) and b (a) is a pseudoscalar (1S_0 state), Van Royen and Weisskopf assume a quark spin-flip electromagnetic $M1$ transition, leading to the reaction $V(P) \rightarrow P(V) + \gamma$. Computed in a nonrelativistic approximation, this gives reasonable results for the decays $V \rightarrow P + \gamma$, in particular for the decay rate of $\omega \rightarrow \pi + \gamma$. Form-factor effects are neglected in the calculation of Van Royen and Weisskopf.

Two-photon decays of pseudoscalar states may be calculated by coupling the photon emission process of Fig. 1 with the vector-dominance hypothesis, whereby a vector meson converts into a photon as in Fig. 2 (note that the vector meson is far off its mass shell).

The effective interaction Hamiltonian for the process is given by³

$$H = ef_{V\gamma} m_V^2 V_\mu A_\mu, \quad (1)$$

where $f_{V\gamma}$ is the vector-dominance coupling constant (the strength of the vertex in Fig. 2). Empirically,⁴ we have

$$f_{\rho\gamma} \simeq \frac{m_\pi}{m_\rho} = 0.18 \quad (2)$$

($f_{\rho\gamma} \simeq m_\pi/m_\rho$ is an assumption, not a theoretical

result). The ratios of the vector-dominance coupling constants for the ϕ , ω , and ρ are given by⁵

$$f_{\rho\gamma}^2 : f_{\omega\gamma}^2 : f_{\phi\gamma}^2 = 9 : 1 : 1.17. \quad (3)$$

On this basis, Van Royen and Weisskopf obtain good agreement with experiment for the decays $\pi^0 \rightarrow \gamma\gamma$ and $\eta \rightarrow \gamma\gamma$.

I. THE $q\bar{q}$ OSCILLATOR MODEL FOR MESONS

We begin with a summary of the $q\bar{q}$ l -excitation oscillator model for mesons. In this model a given mesonic state is represented by a quark-antiquark pair interacting via harmonic-oscillator forces. The Schrödinger equation for the relative motion of the quarks is

$$\frac{-\hbar^2}{M} \nabla_\rho^2 \psi + \frac{1}{2} \kappa \rho^2 \psi = E \psi, \quad (4)$$

where

$$\rho = \vec{r}_2 - \vec{r}_1, \quad \frac{M}{2} = \frac{m_1 m_2}{m_1 + m_2}. \quad (5)$$

The wave functions which correspond to the equation in ρ are given by the expression

$$\psi_{nlm} = N(\alpha\rho)^l L_K^{l+1/2}(\alpha^2\rho^2) \exp(-\frac{1}{2}\alpha^2\rho^2) Y_l^m(\theta, \phi), \quad (6)$$

where $n = l + 2K$, $K = 0, 1, 2, \dots$ is associated with the number of nodes in the radial wave function, l = orbital angular momentum quantum number, $\alpha^2 = (\frac{1}{2}M\kappa)^{1/2} \hbar^{-1}$, where M is the quark mass for equal-mass quarks. $L_K^{l+1/2}$ are Laguerre polynomials and $Y_l^m(\theta, \phi)$ are the spherical harmonics. The normalization constant N is given by

$$|N|^2 = \frac{2\alpha^3 K!}{\sqrt{\pi(K+l+\frac{1}{2})(K+l-\frac{1}{2}) \dots \frac{3}{2} \times \frac{1}{2}}}. \quad (7)$$

Finally, the energy levels are at $E = (n + \frac{3}{2})\hbar\omega$, with $\omega^2 = 2\kappa/M$.

TABLE I. Quark properties.

	B	I	I_3	Y	S	e_q/e
\mathcal{P}	$\frac{1}{3}$	$\frac{1}{2}$	$\frac{1}{2}$	$\frac{1}{3}$	0	$\frac{2}{3}$
\mathcal{N}	$\frac{1}{3}$	$\frac{1}{2}$	$-\frac{1}{2}$	$\frac{1}{3}$	0	$-\frac{1}{3}$
λ	$\frac{1}{3}$	0	0	$-\frac{2}{3}$	-1	$-\frac{1}{3}$

In Table II we list the lowest mesonic states (corresponding to $l=0$ and 1) and the observed mesons associated with them. The mesons are listed according to the assumed $q\bar{q}$ state and their isotopic-spin value t . The numbers in parentheses are the masses in MeV/ c^2 . The last column is the mixing angle for the observed $t=0$ mesons in terms of the pure SU(3) octet and singlet states.⁶ The wave function for $l=0$ is given by

$$\psi_{1s} = \left(\frac{4\alpha^3}{\sqrt{\pi}}\right)^{1/2} \frac{1}{\sqrt{4\pi}} \exp(-\frac{1}{2}\alpha^2\rho^2), \quad (8)$$

and for $l=1$

$$\psi_{1p} = \frac{1}{\sqrt{3}} \left(\frac{4\alpha^3}{\sqrt{\pi}}\right)^{1/2} \frac{1}{\sqrt{4\pi}} \alpha \vec{\rho} \exp(-\frac{1}{2}\alpha^2\rho^2), \quad (9)$$

where $\vec{\rho} = \sqrt{4\pi} \rho Y_1^m(\Omega_\rho)$.

To fit the parameter α^2 we need the oscillator level spacing $\hbar\omega$, since $\hbar\alpha^2 = \frac{1}{2}M\omega$. As an estimate, we may set this equal to the A_2 - ρ mass difference of approximately 550 MeV. The quark mass is determined from the assumption that the quark magneton is equal to the proton moment (which gives the correct nucleon moments in a nonrelativistic qqq model for the baryons). Adopting natural units ($\hbar = c = 1$)

$$\mu = \mu_p = \frac{eg}{2M} = 0.13 \text{ GeV}^{-1},$$

where μ = quark magneton, μ_p = proton magnetic moment, e = electron charge, M = effective quark mass, and g = half the gyromagnetic ratio (=1 for a Dirac moment). This implies $M/g = 0.34$ GeV. Hence $\alpha^2 = 0.094$ GeV², assuming $g=1$. If we had taken the π - B mass difference for $\omega \sim 1100$ MeV, this would have doubled the value of α^2 , giving $\alpha^2 = 0.188$ GeV². In general, in the calculations which follow, both values of α^2 will be used in order to obtain some feeling for the sensitivity

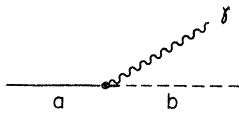


FIG. 1. Diagram for photon emission in processes of the form $a \rightarrow b + \gamma$, where a and b are mesonic $q\bar{q}$ states. The nature of the photonic emission process depends on the spin and orbital angular momentum of $q\bar{q}$ in a and b .

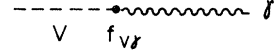


FIG. 2. Vector-dominance diagram for the direct conversion of a vector (1^{--}) meson into a photon.

of the calculations with respect to this parameter.

In Table III we list some selection rules for the decays $a \rightarrow b + \gamma$. In particular a and b cannot both be spinless (no $0 \rightarrow 0$ transitions, rule 9). Furthermore a spin-1 state cannot decay into two photons (rule 4). The other allowed and forbidden transitions are determined by charge-conjugation invariance. For example, an even charge-conjugation state (C^+) can decay into two photons or into a vector meson plus a photon (rules 1 and 5), but not into a π^0 plus a photon (rule 2).

II. THE INTERACTION HAMILTONIAN AND ONE-PHOTON DECAY PROCESSES

The nonrelativistic Hamiltonian corresponding to single quark deexcitation via photon emission has the form

$$H = \sum_{i=1}^2 q^{(i)} (-2ig \vec{S}^{(i)} \cdot \vec{k} \times \vec{A} + 2\vec{P}^{(i)} \cdot \vec{A}) \frac{e}{2M}, \quad (10)$$

where

$$A(\vec{r}^{(i)}) = (4\pi)^{1/2} \left(\frac{1}{2k}\right)^{1/2} \vec{\epsilon} (a_k^\dagger e^{i\vec{k} \cdot \vec{r}^{(i)}} + a_k e^{-i\vec{k} \cdot \vec{r}^{(i)}}). \quad (11)$$

Here $eq^{(i)}$, $\vec{S}^{(i)}$, and $\vec{P}^{(i)}$ are the quark charge, spin, and momentum operators of the i th quark, M is the quark mass, and g is half the gyromagnetic ratio. g is defined by the relation $\mu = eg/2M$, where μ is taken equal to the proton magnetic moment $\mu_p = 0.13$ GeV⁻¹. For a Dirac particle $g=1$. For right circularly polarized photons [$\vec{\epsilon} = -(1/\sqrt{2})(1, i, 0)$] we obtain

$$H' = 2 \left(\frac{\pi}{k}\right)^{1/2} \mu \sum_{i=1}^2 q^{(i)} e^{-ikz^{(i)}} \left(kS_+^{(i)} - \frac{1}{g}P_+^{(i)}\right), \quad (12)$$

where S_+ and P_+ are given by

$$\begin{aligned} S_+ &= S_x + iS_y, \\ P_+ &= P_x + iP_y. \end{aligned} \quad (13)$$

The wave functions of interest for the $ab\gamma$ vertex are given in Sec. I.

We now calculate the space part of the matrix element $\langle 1p | e^{-ikz_1} | 1s \rangle$ and $\langle 1p | e^{-ikz_1} P_{+1} | 1s \rangle$. We find

$$\begin{aligned} \langle 1p | e^{-ikz_1} | 1s \rangle &= \left(\frac{2}{3}\right)^{1/2} \left(\frac{4\alpha^4}{\sqrt{\pi}}\right) \int d^3\rho \rho \exp(-\frac{1}{2}\alpha^2\rho^2) \\ &\quad \times Y_1^{0*}(\Omega) e^{-ikz_1} Y_0^0(\Omega) \end{aligned} \quad (14)$$

TABLE II. Mesonic states (ℓ -excitation model). The numbers in parentheses are the masses in MeV/ c^2 .

$q\bar{q}$ state	J^{PC}	$t=1$	$t=\frac{1}{2}$	$t=0$	$t'=0$	θ
1S_0	0^{-+}	$\pi(137)$	$K(496)$	$\eta(549)$	$\eta'(958)$	11°
3S_1	1^{--}	$\rho(765)$	$K^*(892)$	$\omega(784)$	$\phi(1019)$	40°
1P_1	1^{+-}	$B(1235)$	$K_A(1280-1400)^a$	(1300)		
3P_0	0^{++}	$\left\{ \begin{array}{l} \delta(966) \\ \pi_N(975) \end{array} \right.$	$\left\{ \begin{array}{l} K_N(1080-1260) \\ K(1200-1400) \end{array} \right.$	$\epsilon(\geq 750)$	$S^*(1070)$	
3P_1	1^{++}	$A_1(1070)$	$K_A(1240)^a$	$D(1285)$	$\left\{ \begin{array}{l} \rho\rho(1410) \\ K_s K_s(1440) \end{array} \right.$	
3P_2	2^{++}	$A_2(1310)$	$K_N(1420)$	$f(1260)$	$f'(1514)$	33°

^aThe two $1^+ K_A$ (or Q) states, having identical quantum numbers, are undoubtedly strongly mixed.

$$\langle 1p | e^{-ikz_1} | 1s \rangle = i4\sqrt{2} \frac{\alpha^4}{\sqrt{k}} \int d\rho \rho^{5/2} \exp(-\alpha^2 \rho^2) J_{3/2}(\frac{1}{2}k\rho) \quad (15)$$

$$\langle 1p | e^{-ikz_1} | 1s \rangle = \frac{i}{2\sqrt{2}} \frac{k}{\alpha} \exp\left(\frac{-k^2}{16\alpha^2}\right), \quad (16)$$

where we have applied the identities

$$e^{ikr \cos \theta} = \sum_{l=0}^{\infty} [4\pi(2l+1)]^{1/2} i^l j_l(kr) Y_l^0(\theta), \quad (17)$$

$$j_l(\rho) = \left(\frac{\pi}{2\rho}\right)^{1/2} J_{l+1/2}(\rho), \quad (18)$$

and

$$\begin{aligned} \int_0^\infty dr r^{\nu-1} J_\nu(kr) \exp(-\alpha^2 r^2) \\ = \frac{\Gamma(\frac{1}{2}\nu + \frac{1}{2}) (k/2\alpha)^\nu}{2\alpha^\nu \Gamma(\nu+1)} \\ \times \exp\left(-\frac{k^2}{4\alpha^2}\right) F\left(\frac{1}{2}\nu - \frac{1}{2}\mu + 1, \nu + 1; \frac{k^2}{4\alpha^2}\right). \quad (19) \end{aligned}$$

[$F(a, b, c)$ is the hypergeometric function.] Similarly

$$\begin{aligned} \langle 1p | e^{-ikz_1} P_{+1} | 1s \rangle \\ = -i\left(\frac{2}{3}\right)^{1/2} \left(\frac{4\alpha^4}{\sqrt{\pi}}\right) \int d^3\rho \rho \exp(-\frac{1}{2}\alpha^2 \rho^2) e^{-ikz_1} \\ \times \left(\frac{\partial}{\partial x_1} + i \frac{\partial}{\partial y_1}\right) \\ \times \exp(-\frac{1}{2}\alpha^2 \rho^2) Y_0^0(\Omega) Y_1^{m_1*}(\Omega) \quad (20) \end{aligned}$$

$$\begin{aligned} = i\frac{2}{3} \frac{1}{\sqrt{\pi}} \alpha^6 \int d\rho \rho^4 \exp(-\alpha^2 \rho^2) \int d\Omega Y_1^{m_1*}(\Omega) \\ \times Y_1^1(\Omega) e^{-ikz_1}, \quad (21) \end{aligned}$$

using

$$\begin{aligned} \frac{\partial}{\partial x_1} + i \frac{\partial}{\partial y_1} &= -\left(\frac{\partial}{\partial \rho_x} + i \frac{\partial}{\partial \rho_y}\right) \\ &= -\frac{\partial}{\partial \rho} \sin \theta e^{i\phi} \quad (22) \end{aligned}$$

and noting that

$$Y_1^1(\theta\phi) = -\left(\frac{3}{8\pi}\right)^{1/2} \sin \theta e^{i\phi}.$$

Finally, using

$$Y_1^{1*}(\Omega) Y_1^1(\Omega) = -\frac{1}{\sqrt{20\pi}} Y_2^0(\Omega) + \frac{1}{\sqrt{4\pi}} Y_0^0(\Omega) \quad (23)$$

we find that

$$\begin{aligned} \langle 1p | e^{-ikz_1} P_{+1} | 1s \rangle &= i\frac{2}{3} \frac{\alpha^6}{\sqrt{\pi}} \int d\rho \rho^4 \exp(-\alpha^2 \rho^2) \\ &\quad \times [j_0(\frac{1}{2}k\rho) + j_2(\frac{1}{2}k\rho)] \quad (24) \end{aligned}$$

$$= i\alpha \exp\left(\frac{-k^2}{16\alpha^2}\right). \quad (25)$$

Summarizing, we obtain the two matrix elements: spin

$$\langle 1p | e^{-ikz_1} | 1s \rangle = \frac{i}{2\sqrt{2}} \frac{k}{\alpha} \exp\left(\frac{-k^2}{16\alpha^2}\right) = A, \quad (26)$$

with the selection rule

$$m_1 = 0, \quad m_s = m'_s + 1,$$

and orbital

TABLE III. Selection rules for electromagnetic decays of mesonic states.

(1)	$C^+ \rightarrow \gamma\gamma$	
(2)	$C^+ \rightarrow \pi^0\gamma$	(forbidden by charge conjugation)
(3)	$C^+ \rightarrow \pi^\pm\gamma$	
(4)	$A_1^0 \rightarrow \gamma\gamma$	(forbidden mode for spin-1 particle)
(5)	$C^+ \rightarrow V^0\gamma$	
(6)	$B^\pm \rightarrow \rho^\pm\gamma$	
(7)	$B \rightarrow \pi\gamma$	
(8)	$C^- \rightarrow \pi\gamma$	
(9)	$0 \rightarrow 0$	

$$\langle 1p | e^{-ikz_1} P_{+1} | 1s \rangle = \frac{i\alpha}{g} \exp\left(\frac{-k^2}{16\alpha^2}\right) = B, \quad (27)$$

with the selection rule

$$m_l = +1, \quad m_s = m'_s.$$

We have labeled the first matrix element "spin" to indicate that it corresponds to a spin-flip transition, whereas the second matrix element ("orbital") corresponds to a spin-nonflip process. The g factor is usually taken to be unity (corresponding to no anomalous moment), which gives good agreement between nonrelativistic calculations and experiment.⁷

Finally, for completeness, we give the easily obtained matrix element (space part) for transitions between $1s$ states (vector and pseudoscalar mesons)

$$\langle 1s | e^{-ikz_1} | 1s \rangle = \exp\left(\frac{-k^2}{16\alpha^2}\right), \quad (28)$$

with the selection rule

$$l' = l = 0, \quad m_s = m'_s + 1.$$

As an example consider the decays $A_2 \rightarrow V + \gamma$. The following transitions are allowed: Between the substates $m = +2$ and $m = +1$ there is an allowed transition corresponding to the orbital matrix element (B amplitude) with the expectation value $\langle A_2 | q_1 - q_2 | \rho \rangle = \frac{1}{3}$. The minus sign comes from interchanging quarks 1 and 2 in the space part of the $l=1$ wave function. The appropriate Clebsch-Gordan coefficient = 1. Between the substates $m = +1$ and $m = 0$ there is an orbital transition with $\langle q_1 - q_2 \rangle = \frac{1}{3}$ and Clebsch-Gordan coefficient = $(\frac{1}{2})^{1/2}$ and a spin-flip transition with $\langle A_2 | q_1 S_{+1} - q_2 S_{+2} | \rho \rangle = \frac{1}{3}\sqrt{2}$ and Clebsch-Gordan coefficient = $(\frac{1}{2})^{1/2}$ corresponding to the wave function $\psi_2^{+1} = (\frac{1}{2})^{1/2} Y_1^+ S_1^0 + (\frac{1}{2})^{1/2} Y_1^0 S_1^+$. Finally there is a spin-nonflip transition between the substates $m = 0$ and $m = -1$, with $\langle q_1 - q_2 \rangle = \frac{1}{3}$ and Clebsch-Gordan coefficient = $(\frac{1}{6})^{1/2}$ and a spin-flip transition between these substates with $\langle q_1 S_{+1} - q_2 S_{+2} \rangle = 1/3\sqrt{2}$ and Clebsch-Gordan coefficient = $(\frac{2}{3})^{1/2}$ corresponding to the wave function for $m = 0$:

$$\psi_2^0 = (\frac{1}{6})^{1/2} Y_1^+ S_1^- + (\frac{2}{3})^{1/2} Y_1^0 S_1^0 + (\frac{1}{6})^{1/2} Y_1^- S_1^+.$$

The decay width is given by

$$\begin{aligned} \Gamma_{A_2 \rightarrow \rho + \gamma} &= \frac{1}{4\pi} \frac{4}{2J+1} k^2 \sum |A|^2 \\ &= \frac{8}{45} k \mu^2 \left[\alpha^2 + \left(\frac{-\alpha}{\sqrt{2}} + \frac{1}{4\sqrt{2}} \frac{k^2}{\alpha} \right)^2 \right. \\ &\quad \left. + \left(\frac{-\alpha}{\sqrt{6}} + \frac{1}{2\sqrt{6}} \frac{k^2}{\alpha} \right)^2 \right] \exp\left(\frac{-k^2}{8\alpha^2}\right). \end{aligned} \quad (29)$$

This yields

$$\Gamma_{A_2 \rightarrow \rho + \gamma} = 0.11 \text{ MeV for } \alpha^2 = 0.094 \text{ GeV}^2$$

and

$$\Gamma_{A_2 \rightarrow \rho + \gamma} = 0.29 \text{ MeV for } \alpha^2 = 0.188 \text{ GeV}^2.$$

The width for $A_2 \rightarrow \omega + \gamma$ is similarly obtained (see Table IV) taking into account appropriate SU(3) properties.

To calculate the width for $f \rightarrow V + \gamma$ we take into account the mixing between the SU(3) octet and singlet for the tensor states. We have

$$\begin{aligned} \langle f | q_1 - q_2 | \rho \rangle &= \cos\theta_T \frac{1}{\sqrt{12}} 2 + \sin\theta_T \frac{1}{\sqrt{6}} 2 \\ &= 0.92, \end{aligned} \quad (30)$$

$$\begin{aligned} \langle f | q_1 - q_2 | \omega \rangle &= \frac{1}{3} \langle f | q_1 - q_2 | \rho \rangle \\ &= 0.31, \end{aligned} \quad (31)$$

$$\begin{aligned} \langle f | q_1 - q_2 | \phi \rangle &= -\cos\theta_T \frac{4}{3\sqrt{6}} + \sin\theta_T \frac{2}{3\sqrt{3}} \\ &= 0.24, \end{aligned} \quad (32)$$

where we have assumed $\theta_T = 33^\circ$. Similarly

$$\langle f' | q_1 - q_2 | \rho \rangle = 0.36, \quad (33)$$

$$\langle f' | q_1 - q_2 | \omega \rangle = 0.12, \quad (34)$$

$$\langle f' | q_1 - q_2 | \phi \rangle = 0.61. \quad (35)$$

Substituting the appropriate values in Eq. (29) we obtain the results listed in Table IV.

We may also calculate one-photon decays of the form $M \rightarrow P + \gamma$ ($P =$ pseudoscalar). For example, for $A_2^+ \rightarrow \pi^+ + \gamma$ the only allowed transition is between the substates $m = +1$ and $m = 0$. This is a spin-flip transition (A amplitude) with $\langle A_2^+ | q_1 S_{+1} - q_2 S_{+2} | \pi^+ \rangle = -1/\sqrt{2}$ and the Clebsch-Gordan coef-

TABLE IV. Computed one-photon decay widths.

Decay	$\Gamma(\alpha^2 = 9.4 \times 10^{-2} \text{ GeV}^2)$ (MeV)	$\Gamma(\alpha^2 = 1.88 \times 10^{-1} \text{ GeV}^2)$ (MeV)
$A_2 \rightarrow \rho + \gamma$	0.11	0.29
$A_2 \rightarrow \omega + \gamma$	0.84	2.5
$f \rightarrow \rho + \gamma$	0.84	2.2
$f \rightarrow \omega + \gamma$	0.096	0.24
$f \rightarrow \phi + \gamma$	0.048	0.10
$f' \rightarrow \rho + \gamma$	0.13	0.36
$f' \rightarrow \omega + \gamma$	0.014	0.040
$f' \rightarrow \phi + \gamma$	0.37	0.96
$A_2^+ \rightarrow \pi^+ + \gamma$	0.60	0.40
$A_1^+ \rightarrow \pi^+ + \gamma$	0.40	0.24
$B \rightarrow \pi + \gamma$	0.16	0.44
$\omega \rightarrow \pi^0 + \gamma$	1.1	1.2
$A_1 \rightarrow \rho + \gamma$	0.13	0.25
$A_1 \rightarrow \omega + \gamma$	1.2	2.2
$B^+ \rightarrow \rho^+ + \gamma$	0.20	0.11
$\pi_N \rightarrow \rho + \gamma$	0.10	0.19
$\pi_N \rightarrow \omega + \gamma$	0.80	1.5

ficient $= (\frac{1}{2})^{1/2}$. The spin-nonflip amplitude vanishes due to the orthogonality of the singlet- and triplet-spin matrix elements. The decay width is given by

$$\begin{aligned}\Gamma_{A_2^\pm \rightarrow \pi^\pm + \gamma} &= \frac{1}{4\pi} \frac{4}{2J+1} k^2 \sum |A|^2 \\ &= \frac{k^5 \mu^2}{20\alpha^2} \exp\left(\frac{-k^2}{8\alpha^2}\right) \\ &= 0.60 \text{ MeV for } \alpha^2 = 0.094 \text{ GeV}^2 \\ &= 0.40 \text{ MeV for } \alpha^2 = 0.188 \text{ GeV}^2. \quad (36)\end{aligned}$$

For the decay $A_1^\pm \rightarrow \pi^\pm + \gamma$ the width is given by

$$\Gamma_{A_1^\pm \rightarrow \pi^\pm + \gamma} = \frac{k^5 \mu^2}{12\alpha^2} \exp\left(\frac{-k^2}{8\alpha^2}\right), \quad (37)$$

corresponding to the values given in Table IV.

Finally, for the decay $B^\pm \rightarrow \pi^\pm + \gamma$ we have only a nonflip (B amplitude) transition between the substates $m = +1$ and $m = 0$. The expectation value $\langle B^\pm | q_1 - q_2 | \pi^\pm \rangle = \frac{1}{3}$ and the appropriate Clebsch-Gordan coefficient = 1. Therefore

$$\Gamma_{B^\pm \rightarrow \pi^\pm + \gamma} = \frac{8}{27} k \mu^2 \alpha^2 \exp\left(\frac{-k^2}{8\alpha^2}\right) \quad (38)$$

(see Table IV).

As a test of the model we consider the observed decay $\omega^0 \rightarrow \pi^0 + \gamma$. We find for the width

$$\begin{aligned}\Gamma_{\omega \rightarrow \pi + \gamma} &= \frac{4}{3} k^3 \mu^2 \exp\left(\frac{-k^2}{8\alpha^2}\right) \\ &= 1.1 \text{ MeV for } \alpha^2 = 0.094 \text{ GeV}^2 \\ &= 1.2 \text{ MeV for } \alpha^2 = 0.188 \text{ GeV}^2, \quad (39)\end{aligned}$$

both in good agreement with experiment.⁸

Note, in Table IV, the strong dependence of the decay widths on α^2 , except for the one well-measured decay, $\omega \rightarrow \pi + \gamma$. In contrast to all the others, the decay widths for the processes $A_1^\pm, A_2^\pm \rightarrow \pi^\pm + \gamma$ and $B^\pm \rightarrow \rho^\pm + \gamma$ decrease as α^2 is increased due to the factor $1/\alpha$ which appears in the matrix elements for these spin-flip processes.

The only other case (beside $\omega \rightarrow \pi + \gamma$) that can be compared with an existing experiment, and which is therefore a result of particular interest, is for the process $A_2^\pm \rightarrow \pi^\pm + \gamma$, with $\Gamma(\text{predicted}) = 0.4 - 0.6$ MeV. Eisenberg⁹ *et al.* observed production of the A_2 meson in the reaction $\gamma + p \rightarrow n + \pi^+ + \pi^+ + \pi^-$. Assuming a model in which the A_2 production is due to one-pion exchange, they estimate the width $\Gamma(A_2^\pm \rightarrow \pi^\pm + \gamma)$ to be approximately 0.5 MeV, in excellent agreement with our calculation. Since the calculated width for this decay is the least sensitive to the parameter α^2 , this observation also does not help to limit the permitted range of choice of α^2 .

III. TWO-PHOTON DECAYS OF MESON RESONANCES

We will now calculate decay processes of the form $C^+ \rightarrow \gamma\gamma$ following the model of Van Royen and Weisskopf.² We assume the Feynman diagram for the process as shown in Fig. 3. (C^+ is a neutral nonstrange meson of positive charge conjugation.) The coupling at vertex 1 is given by the nonrelativistic Hamiltonian as in Sec. II, Eqs. (10) and (11) for one-photon decay processes. The coupling at vertex 2 is given by vector dominance. The amplitude corresponding to Fig. 3 is

$$A'_{C^+ \gamma \gamma} = \sum_V A_{C^+ V \gamma} f_{V \gamma}, \quad (40)$$

where $f_{V \gamma}$ is the vector-dominance coupling constant.¹⁰ As an example we calculate the decay $A_2 \rightarrow \gamma\gamma$ in this model. At the first vertex ($A_{A_2 V \gamma}$), the permitted decays are spin-nonflip (orbital) transitions between the substates, with $m = +2$ and $m = +1$, and between the substates $m = 0$ and $m = -1$. (There is no allowed transition between the substates $m = +1$ and $m = 0$ since this would yield a photon of spin projection zero, which violates gauge invariance.) The amplitudes $A_{A_2 V \gamma}$ have been given in Sec. II, while the vector-dominance amplitudes $f_{V \gamma}$ are given by Eqs. (2) and (3). Using these, we find for the width

$$\begin{aligned}\Gamma_{A_2 \rightarrow \gamma\gamma} &= \frac{k^2}{4\pi} \frac{1}{2J+1} (|A'_{A_2 \rightarrow +1}|^2 + |A'_{A_2 \rightarrow -1}|^2 \\ &\quad + |A'_{A_2 \rightarrow -1} + A'_{A_2 \rightarrow +1}|^2) \\ &= \frac{k^2}{4\pi} \frac{1}{2J+1} (2|A_{A_2 \rightarrow +1}|^2 + 4|A_{A_2 \rightarrow -1}|^2) \\ &\quad \times (f_{\rho\gamma} + 3f_{\omega\gamma})^2 e^2 \\ &= \frac{k \mu^2}{45} \left[2\alpha^2 + 4 \left(\frac{-\alpha}{\sqrt{6}} + \frac{1}{2\sqrt{6}} \frac{k^2}{\alpha} \right)^2 \right] 4f_{\rho\gamma}^2 e^2 \\ &\quad \times \exp\left(\frac{-k^2}{8\alpha^2}\right). \quad (41)\end{aligned}$$

The factor of 3 in $(f_{\rho\gamma} + 3f_{\omega\gamma})^2 e^2$ comes from the form of the $q\bar{q}$ isospin combinations for ρ and ω . Substitution into Eq. (41) yields the values shown in Table V.

The f and f' decays into two photons can be calculated from Eq. (41) but taking into account the appropriate SU(3) properties of the two vertices

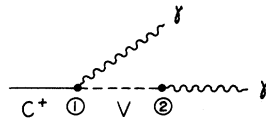


FIG. 3. Diagram for the two-photon decay of positive-charge-conjugation mesons.

[see Eqs. (30)–(35)]. The results are also listed in Table V.

For the 1^+ member of the $l=1, S=1$ mesons, $\Gamma_{A_1 \rightarrow \gamma\gamma} = 0$, since a spin-1 meson cannot decay into two photons.¹¹

Finally we have calculated the decay $\pi_N \rightarrow \gamma\gamma$, where $\pi_N(975 \text{ MeV}) = \delta$ is the 0^+ member of the $l=1, s=1$ multiplet, with wave function

$$\psi_0^0 = \left(\frac{1}{3}\right)^{1/2} Y_1^+ S_1^- - \left(\frac{1}{3}\right)^{1/2} Y_1^0 S_1^0 + \left(\frac{1}{3}\right)^{1/2} Y_1^- S_1^+.$$

We obtain

$$\begin{aligned} \Gamma_{\pi_N \rightarrow \gamma\gamma} &= \frac{k^2}{4\pi} \frac{4}{2J+1} |A_{0 \rightarrow -1}^0|^2 \\ &= \frac{4k\mu^2}{27} \left(\alpha + \frac{k^2}{4\alpha}\right)^2 \exp\left(\frac{-k^2}{8\alpha^2}\right) 4f_{\rho\gamma}^2 e^2, \end{aligned} \quad (42)$$

and the values are given in Table V.

It is useful, as a check on the model, to calculate also the decays $\pi^0 \rightarrow \gamma\gamma$ and $\eta \rightarrow \gamma\gamma$ in this model. Consider the decay $\pi^0 \rightarrow \gamma\gamma$. The transition $\pi \rightarrow V\gamma$ is a magnetic dipole ($M1$) transition. The spatial matrix element is given by Eq. (28):

$$\langle 1s | \exp(-ikz_1) | 1s \rangle = \exp\left(\frac{-k^2}{16\alpha^2}\right),$$

while the expectation value $\langle \pi | q_1 S_{+1} + q_2 S_{+2} | \rho \rangle = 1/3\sqrt{2}$. Therefore the width is given by

$$\begin{aligned} \Gamma_{\pi^0 \rightarrow \gamma\gamma} &= \frac{k^2}{4\pi} \frac{4}{2J+1} |A_{0 \rightarrow -1}^0|^2 \\ &= \frac{1}{9} m_\pi^3 \mu^2 e^2 f_{\rho\gamma}^2 \exp\left(\frac{-k^2}{8\alpha^2}\right), \end{aligned} \quad (43)$$

with the results given in Table V. The values are approximately the same for the two values of α^2 since the form factor is ~ 1 for the small value of k^2 .

For the case of the η we have

$$\eta = \eta_8 \cos 11^\circ + \eta_1 \sin 11^\circ, \quad (44)$$

where

$$\eta_8 = \frac{1}{\sqrt{6}} (\phi\bar{\phi} + \mathfrak{N}\bar{\mathfrak{N}} - 2\lambda\bar{\lambda}) \quad (45)$$

TABLE V. Computed two-photon decay widths.

Decay	$\Gamma(\alpha^2 = 9.4 \times 10^{-2} \text{ GeV}^2)$	$\Gamma(\alpha^2 = 1.88 \times 10^{-1} \text{ GeV}^2)$
$A_0^0 \rightarrow \gamma\gamma$	0.46 keV	0.81 keV
$f(1260) \rightarrow \gamma\gamma$	1.2 keV	2.3 keV
$f'(1514) \rightarrow \gamma\gamma$	0.14 keV	0.19 keV
$A_1^0 \rightarrow \gamma\gamma$	0	0
$\pi_N(975) \rightarrow \gamma\gamma$	2.5 keV	3.8 keV
$\pi^0 \rightarrow \gamma\gamma$	13 eV	13 eV
$\eta \rightarrow \gamma\gamma$	1.7 keV	1.8 keV

and

$$\eta_1 = \frac{1}{\sqrt{3}} (\phi\bar{\phi} + \mathfrak{N}\bar{\mathfrak{N}} + \lambda\bar{\lambda}). \quad (46)$$

Thus

$$\begin{aligned} \langle \eta | q_1 S_{+1} + q_2 S_{+2} | \rho \rangle &= \cos 11^\circ \frac{1}{\sqrt{12}} 2 + \sin 11^\circ \frac{1}{\sqrt{6}} 2 \\ &= 0.72. \end{aligned} \quad (47)$$

Similarly

$$\langle \eta | q_1 S_{+1} + q_2 S_{+2} | \omega \rangle = 0.24 \quad (48)$$

and

$$\langle \eta | q_1 S_{+1} + q_2 S_{+2} | \phi \rangle = -0.45. \quad (49)$$

Hence

$$\begin{aligned} \Gamma_{\eta \rightarrow \gamma\gamma} &= \frac{1}{2} m_\eta^3 \mu^2 \exp(-k^2/8\alpha^2) \\ &\times \left| \sum_V \langle \eta | q S_+ | V \rangle f_{V\gamma} \right|^2 e^2 \end{aligned} \quad (50)$$

($m_\eta = \eta$ mass) giving the results in Table V.

Referring to Table V, we observe a rather strong dependence on α^2 for the decays of tensor mesons but only the slightest α^2 dependence for the decays of the pseudoscalar mesons. Notice that the decay $f'(1514) \rightarrow \gamma\gamma$ is suppressed due to SU(3) considerations. The numbers for the pseudoscalar meson decays agree with experiment to better than within a factor of ~ 2 . Experimentally,¹² $\Gamma_{\pi^0 \rightarrow \gamma\gamma} = 7.8 \pm 0.9$ eV and $\Gamma_{\eta \rightarrow \gamma\gamma} = 1.0 \pm 0.3$ keV.

For comparison purposes Kunzst *et al.*¹³ compute $\Gamma_{f \rightarrow \gamma\gamma} = 6.6$ keV.¹⁴ This calculation is based on the assumed phenomenological Lagrangian

$$\mathcal{L}_{\text{int}}(x) = \frac{g}{m_f} G_{\mu\nu} F^{\mu\lambda} F_{\lambda\nu} + \frac{f}{m_f} G_{\mu\nu} \partial^\mu \pi \partial^\nu \pi \quad (51)$$

for the $f\gamma\gamma$ and $f\pi\pi$ vertices with couplings g and f , respectively, where $G_{\mu\nu}$ is the spin-2 field operator, $F_{\mu\nu} = \partial_\mu A_\nu - \partial_\nu A_\mu$ (A_μ is the photon vector potential), and π is the pion field. A universality hypothesis requires the hadrons to be coupled to the symmetric energy-momentum tensor with the same strength:

$$\Theta_{\mu\nu} = \frac{f}{m_f} (\partial_\mu \pi \partial_\nu \pi + V_{\mu\lambda} V_{\lambda\nu} + \dots), \quad (52)$$

where $\Theta_{\mu\nu}$ is the stress-energy tensor and $V_{\mu\lambda} = \partial_\mu V_\lambda - \partial_\lambda V_\mu$. Finally, the vector-dominance hypothesis is applied to connect V_μ and A_μ , yielding the result quoted above for the width $\Gamma_{f\gamma\gamma}$ (based on the experimental value for $\Gamma_{f\pi\pi}$).

Reviewing our results for one- and two-photon decays of meson resonances in the quark-oscillator model, we find the usual good agreement with experiment for decays of $l=0$ states (for example,

$\omega \rightarrow \pi\gamma$, $\pi^0 \rightarrow \gamma\gamma$, and $\eta \rightarrow \gamma\gamma$). These results are not very sensitive to the well-width parameter α^2 . Calculations for $l=1$ resonances decaying via radiative emission are quite sensitive to the value of α^2 in general. The prediction for $A_2^+ \rightarrow \pi^+ + \gamma$ [$\Gamma(\text{predicted}) = 0.4-0.6$ MeV] is in good agreement with the experimental value $\Gamma(\text{experimental}) \sim 0.5$ MeV.

On the other hand, our calculations give a prediction for the decay width of $f(1260) \rightarrow \gamma\gamma$ which is lower than the value predicted by Kunzst *et al.*

on the basis of a phenomenological Lagrangian by at least a factor of three. It will, therefore, be interesting to obtain experimental information on this decay width as a test of models. We conclude with the remark that, although the quark model gives good agreement with experiment for radiative decays of low-lying meson states, more experimental information is needed to test the validity of the quark-oscillator model for the decays of more highly excited mesonic states such as the tensor mesons.

*This work is supported in part through funds provided by the Atomic Energy Commission under Contract No. AT(11-1)-3069.

¹See, e.g., B. T. Feld, *Models of Elementary Particles* (Ginn, Boston, Mass., 1969) for a review.

²R. Van Royen and V. F. Weisskopf, *Nuovo Cimento* **50**, 617 (1967).

³Y. Nambu and J. J. Sakurai, *Phys. Rev. Lett.* **8**, 79 (1962).

⁴M. Gell-Mann and F. Zachariasen, *Phys. Rev.* **124**, 953 (1961).

⁵SU(3) predicts 9:1:2 for the ratios in Eq. (3). The relative decrease of $f_{\phi\gamma}^2$ is due to the heavier mass of the ϕ meson through the assumption [cf. Eq. (2)] $f_{V\gamma} \propto m_\pi/m_V$.

⁶B. T. Feld, in *Fundamental Interactions at High Energy*, edited by T. Gudehus *et al.* (Gordon and Breach, New York, 1969).

⁷J. Kokkedee, *The Quark Model* (Benjamin, New York, 1969).

⁸The 1972 Tables of Particle Properties [Particle Data Group, *Phys. Lett.* **39B**, 1 (1972)] give $\Gamma_{\omega \rightarrow \pi^0 \gamma} = 0.90 \pm 0.06$ MeV.

⁹Y. Eisenberg *et al.*, *Phys. Rev. Lett.* **23**, 1322 (1969).

¹⁰Some authors use the constant $\gamma_V = 1/2 f_{V\gamma}$.

¹¹It has been proved by E. P. Wigner that the two-photon decay of a vector meson of either parity is forbidden by angular momentum conservation requirements. See J. Steinberger, *Phys. Rev.* **76**, 1180 (1949).

¹²1972 Tables of Particle Properties, Ref. 8.

¹³Z. Kunzst, R. M. Muradyan, and V. M. Ter-Atonyan, Dubna Report No. E2-5424, 1970 (unpublished).

¹⁴Kunzst *et al.* predict 8 keV in their paper, but they assumed a value for $\Gamma_{f \rightarrow \pi\pi}$ which is too high according to recent experiments.

Perturbative Treatment of Threshold Contributions to a Rising pp Total Cross Section*

T. K. Gaisser[†]

Bartol Research Foundation of The Franklin Institute, Swarthmore, Pennsylvania 19081

Chung-I Tan

Brookhaven National Laboratory, Upton, New York 11973

and Department of Physics, Brown University[‡], Providence, Rhode Island 02912

(Received 23 July 1973)

We analyze the relation between increasing $N\bar{N}$ production and increasing σ_{tot} in a two-component picture. The possible increasing contribution to the cross section of diffractive dissociation into high-mass states is taken into account. We conclude that it is likely that both effects are important at CERN ISR energies. We also find that the short-range correlation part of the inelastic cross section without $N\bar{N}$ production must decrease above $s \sim 150$ GeV². The decrease is consistent with the form $\sigma^{(0)} \propto s^{\alpha_0 - 1}$ with $\alpha_0 = 0.92 \pm 0.04$.

I. INTRODUCTION

A possible explanation of the rise in the pp total cross section over the CERN ISR energy range^{1,2} ($500 \leq s \leq 3000$ GeV²) is the presence of threshold

effects. For example, within the context of a two-component model, Chew and others have shown that the contribution to σ_{tot} of single diffractive dissociation into high missing mass (M) exhibits a logarithmic threshold increase with energy.³⁻⁵